IOSR Journal of Environmental Science, Toxicology and Food Technology (IOSR-JESTFT)
e-ISSN: 2319-2402, p- ISSN: 2319-2399.Volume 19, Issue 6 Ser. 2 (June 2025), PP 48-59
www.iosrjournals.org

Bio-sorption of Fuschin Basic Using *Datura stramonium* Leaves as Adsorbent

Maty Mossane Diouf, Ramatoulaye Diouf, Aïssatou Alioune Gaye*, Alioune Fall

Department of Chemistry, Faculty of Sciences and Technology, University Cheikh Anta Diop, Dakar, 10700, Sénégal

Abstract:
Fuschin basic dye was adsorbed on an adsorbent prepared from leaves of the Datura stramonium. A batch adsorption study was carried out with variable adsorbate concentration, adsorbent amount, particle size of the adsorbent, pH, and time of contact. From 50 mL of 50 ppm aqueous solution of fuchsin basic, 96.51% of the dye could be removed by 0.25 g of adsorbent (leaf powder of Datura stramonium) at 298 K, after 60 minutes of stirring. The optimum parameters such as contact time, particle size, absorbent dose, initial fuschin basic concentration, and pH were investigated by performing batch experiments models. The optimum of contact time is 60min, with a removal capacity of 96.51 %. The optimal adsorbent concentration to reach the maximum removal of fuschin basic is 14 g/L with a removal capacity of 96.51 %. An initial fuschin basic concentration of 70 ppm is ideal to reach the maximum capacity of removal (97.00 %). The optimum particle size is 125 µm with 96.84 % of removal capacity and the optimal pH value is 5 with 95.27 % of dye removal. The kinetics of the adsorption process are in accordance with the pseudo-second order model. The kinetics and the isotherms adsorption were evaluated by varying the initial concentration and using the optimum parameters. Experimental values of the adsorption capacity are close proximity to the optimum values predicted by the pseudo-second order model. Langmuir, Freundlich, Temkin, Dubinin-Radushkevich, Harkin-Jura and Hasley isotherms were applied to represent the data obtained from the adsorption studies. The highest R^2 values were related to Temkin (94.9 %) and Dubinin-Radushkevich (96.5 %) models.
Keywords: *Dye, Isotherm, Kinetic, Adsorption, Basic Fuschin, Datura stramonium.*

Date of Submission: 03-06-2025 Date of Acceptance: 13-06-2025

I.Introduction

Basic fuchsin (BF) is a fluorescent dye that is a mixture of rosaniline, pararosaniline, new fuchsin, and magenta II. It is widely used in the textile and leather industry [1]. It is also involved in the detection of certain acid-fast microorganisms [2]. These industries discharge large quantities of basic fuschin contaminated wastewater into the environment. Due to their low biodegradability, the dyes can accumulate in surface water and sediments and end up in the food chain. This can be dangerous for the environment and human and animal health [3]. Indeed, the coloring of water can seriously affect the phenomenon of photosynthesis and inhibit the normal development of aquatic plants and animals [4]. Additionally, the degradation of these dyes can lead to the formation of toxic compounds [5–7] which can lead to the development of adverse effects such as dizziness, vomiting, diarrhea or respiratory irritation [8]. Exposure to organic dyes can cause carcinogenic or mutagenic effects [9]. Methods for decontaminating industrial wastewater are very varied. There are biological treatment methods, by chemical coagulation and by adsorption on activated carbon [10–13]. Activated carbon treatment has proven highly effective in decontaminating dye-laden water due to its excellent surface properties and high adsorption capacity [14, 15]. However, this method is quite expensive due to adsorbent regeneration issues [10, 16]. Other wastewater treatment methods, such as electrochemical, ion exchange, or catalytic reduction processes, have limitations in effectively removing cationic dyes [17]. These methods are expensive due to longer treatment time, expensive maintenance, high energy consumption, and rapid catalyst deactivation, low decontamination rate, and waste production [18, 19]. Alternative solutions with low-cost adsorbents are being sought to decontaminate contaminated water. These adsorbents include sources from agro-industrial waste and biomass by-products [20–24]. The present study investigated the removal of basic fuchsin from aqueous solution using Datura stramonium leaves as an effective, available, and inexpensive adsorbent.

* Corresponding author: aissatoualioune.gaye@ucad.edu.sn

II.Material and methods

Preparation of the adsorbent

Datura stramonium was harvested at Mbetit Gouye (Fatick Region in Senegal 14°25'59.99''N, 16°31'59.99''O). *Datura stramonium* leaves (DSL) were collected and rinsed twice with tap water first and distilled water to remove all the particles. They were shadow dried for three days. After this first process, the DSL were dried at 50°C for 48 hours and ground using a grinder. The resulting powder was stored in a plastic container until use. The dried DSL adsorbent was again crushed and sieved to get different sized fractions, namely, 80, 100, 125, 250, 315, 400, 500, 1500 µm. These different fractions were stored in airtight containers for further use.

FTIR and UV-Visible analysis

The FTIR spectra of the prepared sample were recorded on a FTIR Spectrum Two of Perkin Elmer (4000–400 cm^{-1}). The residual fuschin basic concentration was determined using a Perkin-Elmer UV/Visible spectrophotometer Lambda 365 (1000–200 nm).

Point zero charge pH_{PZC}

The pH of the point of zero charge (pH_{PZC}) for the *Datura stramonium* leaves (DSL) was determined by a titration procedure. To a series of eleven 150 mL conical flasks 45 mL of a solution of KNO_3 0.01 M were added and the pH was accurately adjusted using HCl or NaOH 0.01 N solutions from pH = 2 to pH = 12 and completed with a solution KNO_3 0.01 M to 50 mL. The initial pH (pH_i) was accurately measured again. To each flask, 0.1 g of DSL was added, and the flask was capped and shaken manually each 4 hours. After 48 hours, the final pH (pH_f) was measured. The $\Delta pH = pH_f - pH_i$ is plotted against pH_i. The point of intersection of the curve and the abscissa axe at pH = 0 gave the pH_{PZC}.

Batch adsorption tests

All the experiments were conducted in discontinuous batch. A weighed sample of DSL was mixed with 50 mL of the fuschin basic (scheme 1) solution in 150 mL conical flasks. The mixture was stirred for a fixed time at 25°C. After this process, the liquid was separated from the adsorbent by filtration through a Whatman Filter N°1. The experimental data were used to determine the removal capacity, and the quantity of fuschin basic adsorbed on the DSL:

$$Removal\ \ capacity = \frac{(C_0 - C_e) \times V}{C_0} \times 100$$

$$q_e = \frac{(C_0 - C_e) \times V}{m}$$

Where C_0 and C_e are respectively the initial and the final metal concentrations (mg/L) in the liquid phase, V (L) is the volume of the liquid phase and m (g) is the adsorbent mass used.

Effect of time contact on the removal capacity

The equilibrium time was determined using a Fuschin basic solution at a concentration of 50 ppm. Each 50 mL Fuschin basic solution was treated with 0.25 g of DSL at time ranging from 10 to 180 minutes. The experiments were conducted at the same pH and the flasks contents were stirred at 500 rpm at a temperature of 25°C.

Adsorbent dose effect on the removal capacity

50 mL of a 50 ppm fuschin basic solution was treated with a mass of adsorbent ranging from 0.1 to 1.0 g. The experiments were conducted at the same pH and the flasks contents were shaken at 500 rpm at temperature of 25°C for the optimal time determined previously.

Effect of adsorbent particle size on the removal capacity

The ideal particle size for the adsorbent was determined by treating each category (80,100, 125, 250, 315, 400, 500 and 1500 µm) with 50 mL of a 50 ppm Fuschin basic solution at the optimum pH using 0.9 g of DSL powder. The flasks were shaken at 500 rpm and at a temperature of 25°C for the optimal time determined previously.

Effect of solution pH on the removal capacity

The effect of solution pH on the dyes removal capacities of the adsorbent was investigated between pH = 2 and pH = 11. The experiments were performed by adding a 0.9 g of DSL powder (particle size 80 µm) into six 150 mL conical flasks containing 50 mL of 50 ppm dye solutions and the pH of the solution was adjusted using 0.1 N

HCl or 0.1 N NaOH. The flasks were shaken at 500 rpm and at temperature of 25°C for the optimal time determined previously.

Effect of fuschin basic solution concentration on the removal capacity

The effect of concentration of fuschin basic solution on the removal capacity were determined by setting the optimum parameters : time, granulometry of the adsorbent, dose of the adsorbent and pH of the solution and varying the fuschin basic concentration between 10 to 100 ppm. The flasks content were stirred at 500 rpm at a temperature of 25°C for the optimal time determined previously.

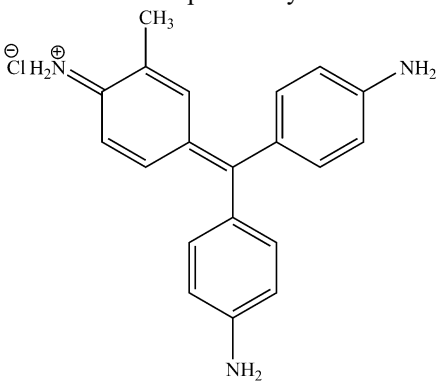

Scheme 1. Structural formulae of fuschin basic.

III.Results and discussion

FTIR spectral analysis

Fourier transform infrared spectroscopy (FTIR) is a functional analysis tool that can identify the main functions in organic chemistry, particularly according to their vibration modes. It is a technique that can determine the presence of compounds in samples by collecting the vibrational modes of the chemical functions that characterize them. In order to determine the existence of interactions between the adsorbent (DSL) and the adsorbate (Fuschin), the FTIR spectra of the pure adsorbent and the adsorbent impregnated by the adsorbate (DSL-F) are recorded (Fig. 1). The spectrum of the pure adsorbent shows a broad band at 3282 cm^{-1} which is due to the ν_{O-H} stretching [25]. The intense band at 1634 cm^{-1} is attributed to the $\nu_{C=O}$ stretching (amide-I band) O=C-NHR while the low intensity band obtained at 1317 cm^{-1} corresponds to the N-H bending. The bands at 2919 and 2850 cm^{-1} were assigned to the ν_{Csp^3-H} vibration. At 1238 cm^{-1} a band assigned do δ_{O-H} is observed. The δ_{C-O} stretching band vibrations are observed at 1104 cm^{-1} and 1022 cm^{-1} [26]. The FT-IR spectrum of the adsorbent impregnated by the adsorbate (DSL-BF) shows bands similar to those found in the DSL spectrum with very small shifts for the absorption band values and intensities of these bands (Fig. 1).

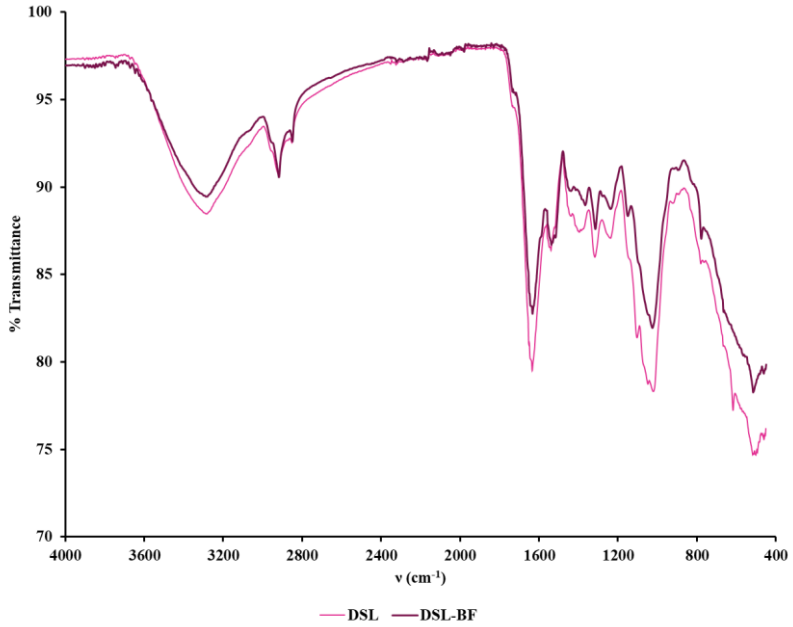

Figure 1. FTIR spectrum of DSL and DSL-BF.

Optimization of the parameters fuschin basic removal

To determine the best conditions for adsorption of fuschin basic using *Datura stramonium* leaves (DSL) as adsorbent, certain parameters such as contact time, amount of adsorbent used, particle size, pH or initial concentration of the fuschin basic solution were studied.

The adsorption capacity of *Datura stramonium* leaves is studied as a function of contact time because of the role played by this parameter on the adsorption equilibrium (Figure 2). The initial adsorbate solution of 50 mg/L was used. After 10 minutes, we observed an adsorption rate of 92.44 %. The adsorption rate continues to increase slowly and reaches a maximum of 96.05 % after 60 minutes. Subsequently, the adsorption rate fluctuates between 96.04 and 96.51 %. For the rest of our study, the contact time is set at 60 minutes.

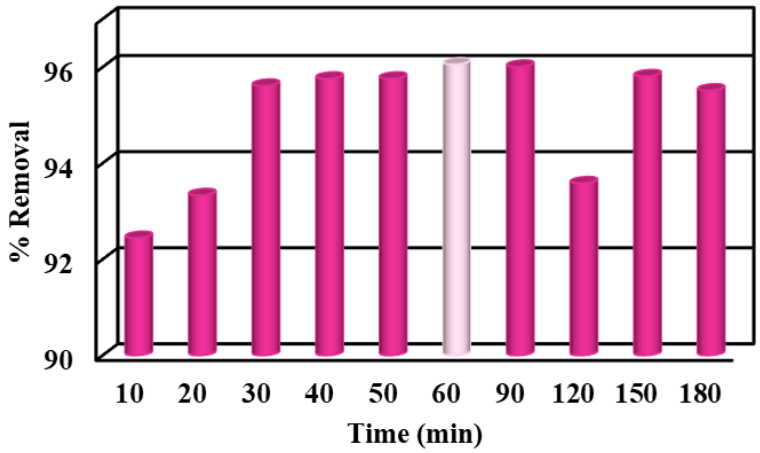

Figure 2. Effect of contact time on the adsorption capacity of DSL.

The adsorbent dose is then studied (Figure 3). The masse of adsorbent is varied at constant volume (50 mL) from 0.1 g to 1 g with a contact time of 60 minutes. The adsorption rates is 80.51 % for an adsorbent mass of 0.1 g. It then increases to 87.30 % between 0.5 and 0.6 g. It reaches a maximum value of 90.36 % at 0.7 g before decreasing to 85.99 % at 1 g. For the rest of the study, the contact time is set at 60 minutes, and the mass of adsorbent is set at 0.7 g for 50 mL of solution.

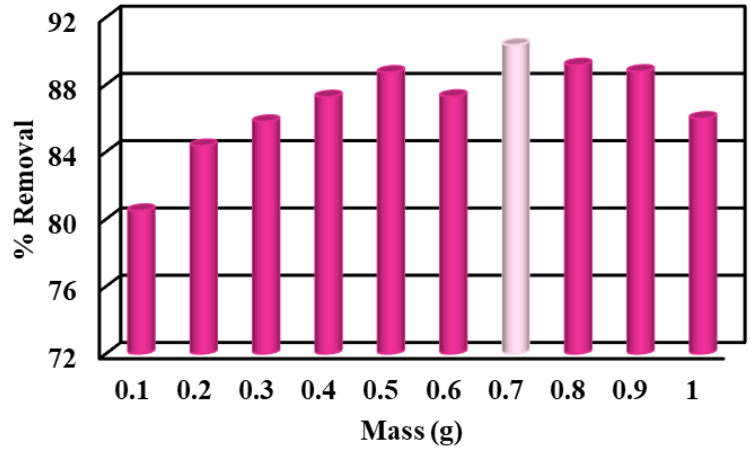

Figure 3. Effect of adsorbent dose on the removal capacity.

The influence of the particle size of the adsorbent on the adsorption rate is studied (Figure 4). An increase in the adsorption rate is observed when the particle size decreases. This phenomenon is probably due to the decrease in specific surface area when the grain size increases. For particle sizes between 100 – 1500 µm, the adsorption rate varies between 95.09 %, and 86.50 %. The maximum adsorption rate (96.84 %) is obtained for the particle size of 125 µm.

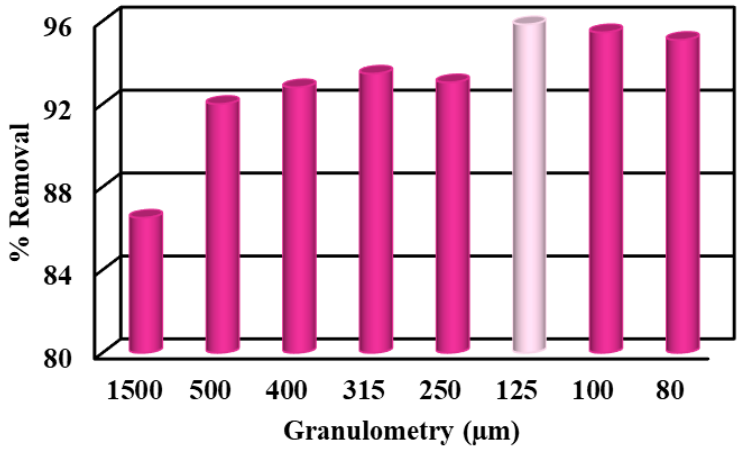

Figure 4. Effect of adsorbent particle size on the removal capacity

The pH study is carried out for a particle size of 125 µm, a mass of 0.7 g for 50 mL of solvent, at 50 mg/L for fuschin basic concentration and a contact time of 60 minutes (Figure 5). The pH of the zero charge point of the adsorbent is determined and is equal to 6.80. The zero charge point pH is the pH for which the charge on the adsorbent surface is zero. The influence of pH on the adsorption rate is significant because pH acts on the surface of the adsorbent and on the adsorbate. When the pH is higher than the zero charge point pH, the surface of the adsorbent is negatively charged, and the cations can easily interact with the surface of the adsorbent. When the pH is lower than the zero charge point pH, the surface of the adsorbent is positively charged, and the anions are well retained on the surface of the adsorbent. Since fuschin basic is cationic, it interacts less well with the adsorbent surface when the latter has a positively charged surface. Indeed, competition with protons leads to a decrease in the number of sites available to fix fuschin basic. Consequently, for strongly acidic pH, the adsorption rate is lower (90.54 %, pH = 2). It increases and reaches 95.27 % at pH = 5. It remains quite constant up to pH = 9 and then decreases sharpy to 82.63% at pH =11.

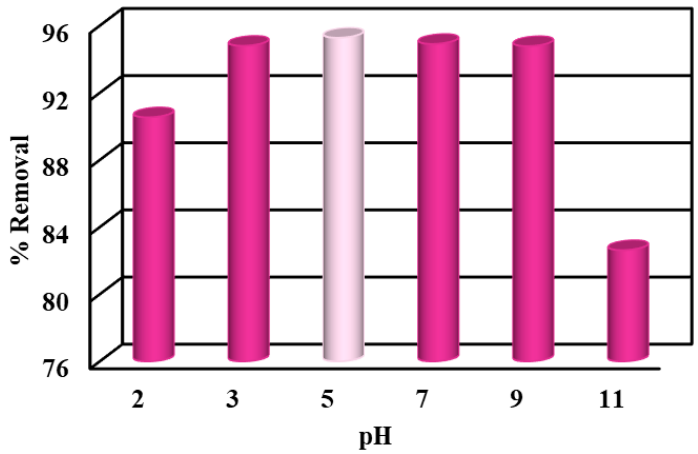

Figure 5. Effect of pH of the solution on the removal capacity.

The adsorption capacity is strongly linked to the initial concentration of the adsorbate in solution. Figure 6 shows that the lowest adsorption capacity is lowest for initial concentration of fuschin basic of 10 ppm . It increases regularly and reaches its maximum value of 97.00 % for an initial concentration of 70 ppm. Between 80 and 100 ppm the absorption capacity fluctuates between 96.00 and 95.98 %.

Throughout the rest of the study, the following conditions are used: a dose of 0.7 g of adsorbent with particle size of 125 µm, initial adsorbate concentration of 70 ppm and a contact time of 60 minutes at pH = 5.

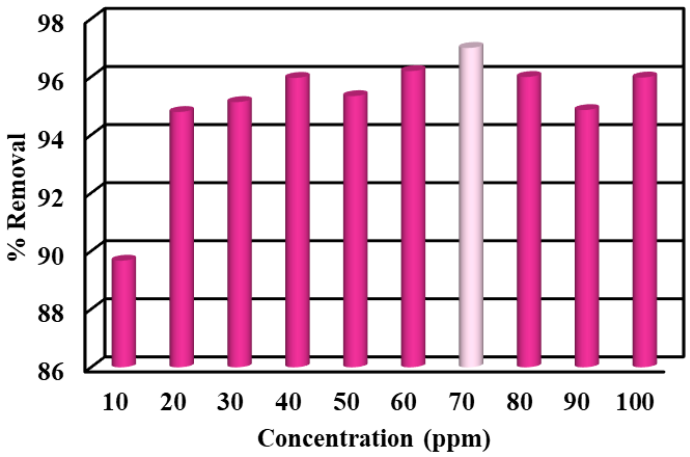

Figure 6. Effect of fuschin basic initial concentration on the removal capacity.

Kinetic aspects

The kinetic studies of the adsorption of fuschin basic on *Datura stramonium* leaf powder are carried out with a pH = 5, a temperature of 25°C, a concentration adsorbent of granulometry of 125 µm of 14 g/L. Different initial concentrations of the adsorbate (10 to 100 ppm) are used. The aqueous concentrations of dyes were measured similarly, varying time contact. The amount of dye adsorbed q_t (mg/g) at time t is calculated using the following equation 1

$$\text{Equation 1: } q_t = \frac{(C_0 - C_t).V}{m_0}$$

where C_t (mg/L) is the aqueous dye concentration at time t, C_o (mg/L) is the initial concentration of dye, V is the volume (L) and m_0 (g) is the weight of adsorbent.

Four kinetic models: pseudo-first-order [27], pseudo-second-order [28], intra-particle diffusion model [29] and Elovich model [30] were examined in order to understand the adsorption mechanism on the leaves powder of *Datura stramonium*. The fit of these models was checked by each linear plot of the representative equation, respectively and by comparing to the regression coefficients for each expression. All the parameters of each model are presented in Table 1.

Pseudo-first-order model

The expression for Pseudo-first-order model proposed by Lagergren [27] is described by equation 2.

$$\text{Equation 2: } Ln(q_e - q_t) = Lnq_e - k_1 t$$

Where q_e is the equilibrium adsorption quantity (mg/g), q_t is the amount of dye adsorbed at time t (mg/g), and k_1 is the rate constant (mn^{-1}).

The plot $Ln(q_e\text{-}q_t)$ *versus t* (Figure 7), gives the values for $q_{e,cal}$, k_1, respectively, from slope and intercept values and R^2 which are reported in Table 1. The $q_{e,cal}$ values don't fit the experimental $q_{e,exp}$ values and the R^2 values are far from the ideal value of 1. These facts are indicative that the pseudo-first-order is not suitable to describe to the adsorption process.

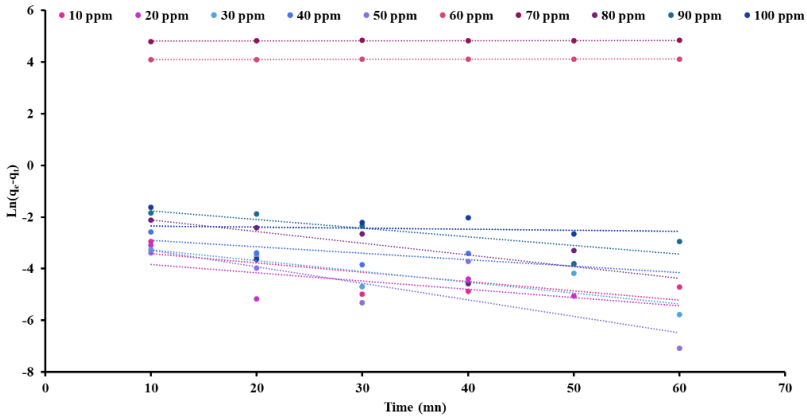

Figure 7. Pseudo-first order Kinetic model for adsorption of fuschin basic on DSL.

Table 1. Kinetic parameters of the adsorption of fuschin basic.

C_0 (ppm)	$q_{e,exp}$ (mg/g)	Pseudo-first order $\ln(q_e - q_t) = \ln q_e - k_1 t$			Pseudo-second order $\frac{t}{q_t} = \frac{1}{k_2 q_e^2} + \frac{1}{q_e} t$		
		k_1 (min^{-1})	$q_{e,cal}$ (mg/g)	R^2	k_2 (g/mg min)	$q_{e,cal}$ (mg/g)	R^2
10	**0.650**	0.036	0.047	0.582	1.781	0.655	0.9997
20	**1.353**	0.032	0.029	0.362	2.297	1.358	1.0000
30	**2.042**	0.042	0.057	0.722	2.135	2.044	0.9999
40	**2.742**	0.025	0.070	0.593	1.040	2.747	0.9999
50	**3.404**	0.064	0.072	0.659	2.019	3.409	1.0000
60	**4.120**	0.053	0.054	0.941	2.082	4.127	1.0000
70	**4.848**	0.051	0.077	0.487	3.439	4.843	1.0000
80	**5.483**	0.045	0.191	0.535	0.491	5.504	0.9999
90	**6.150**	0.034	0.243	0.703	0.467	6.154	0.9999
100	**6.851**	0.004	0.100	0.008	0.420	6.849	0.9997
C_0 (ppm)	$q_{e,exp}$ (mg/g)	Intraparticle Diffusion $q_t = k_i t + I$			Elovich $q_t = \frac{1}{\beta}\ln \alpha\beta + \frac{1}{\beta}\ln t$		
		k_i (mg/g min)	I	R^2	β (g/mg)	α (mg/min)	R^2
10	**0.650**	0.010	0.574	0.778	36.232	8.15×10^{6}	0.864
20	**1.353**	0.008	1.297	0.613	156.250	1.70×10^{87}	0.529
30	**2.042**	0.008	1.981	0.714	49.020	8.93×10^{39}	0.756
40	**2.742**	0.013	2.636	0.786	28.818	9.80×10^{30}	0.829
50	**3.404**	0.007	3.353	0.626	58.824	2.36×10^{83}	0.642
60	**4.120**	0.006	4.074	0.959	65.359	2.08×10^{113}	0.931
70	**4.848**	0.006	4.795	0.351	56.180	4.26×10^{114}	0.427
80	**5.483**	0.026	5.279	0.889	14.993	4.90×10^{32}	0.880
90	**6.150**	0.033	5.880	0.710	11.655	1.51×10^{28}	0.719
100	**6.851**	0.027	6.609	0.387	14.286	3.33×10^{19}	0.642

Pseudo-second-order model

The equation pseudo-second-order model is described by the equation 3 established by Ho and McKay's [28].

$$\text{Equation 3: } \frac{t}{q_t} = \frac{1}{k_2 q_e^2} + \frac{t}{q_e}$$

where q_e is the equilibrium adsorption capacity (mg/g), q_t (mg/g) is the adsorption capacity at time t, k_2 (g/mg min) is the rate constant for the pseudo-first order kinetic model. The plot t/q_t *versus* t gives straight lines for the different initial fuschin basic concentrations (10 ppm to 100 ppm). The parameters $q_{e,cal}$ and k_2 were obtained from the slopes and intercepts of straight lines, and R^2 were calculated and reported in Table 1. The $q_{e,cal}$ values fit the experimental $q_{e,exp}$ value and the R^2 values are close to the unit. These facts are indicative that the pseudo-second-order model is more suitable for the description of the adsorption process.

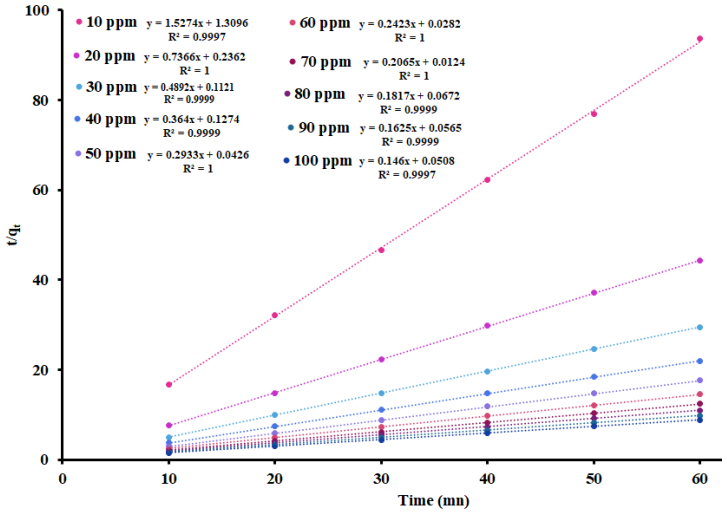

Figure 8. Pseudo-second order Kinetic model for adsorption of fuschin basic on DSL.

Intra-particle diffusion model

The Intra-particle diffusion model is described by the Equation 4 established by Weber and Morris [29].

$$\text{Equation 4: } q_t = k_i t^{1/2} + I$$

The plot of Equation 4 should be linear if intra-particle diffusion is involved in the adsorption mechanism. Additionally intra-particle diffusion is the rate-controlling step, if the straight line passes through the origin. If the straight line does not cross the origin, this is indicative that the intra-particle is not the only rate-controlling step. Figure 9 shows the plots of Equation 4 at different initial fuschin basic concentrations (10 ppm to 100 ppm). All curves are not linear and do not pass though the origin and the correlation coefficients R^2 are very low. These observations are indicative that the intraparticle diffusion in not the rate-controlling step.

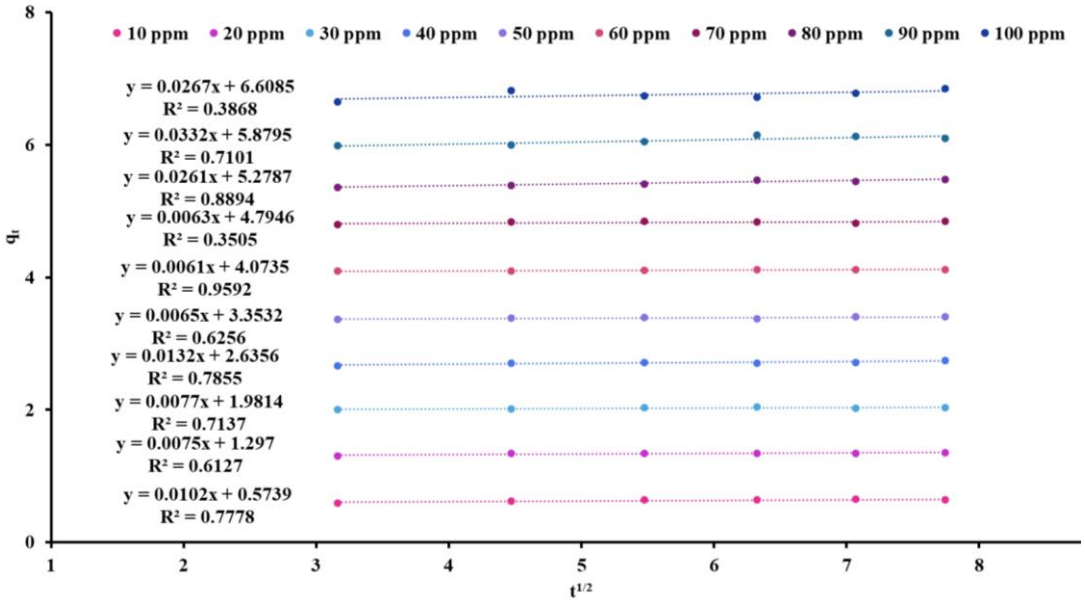

Figure 9. Intraparticle kinetic model for adsorption of fuschin basic on DSL

Elovich model

The kinetic model called Elovich [30] is described by equation 5 which assumes the description of chemisorption on a heterogeneous surface.

$$\text{Equation 5: } q_t = \frac{1}{\beta}\ln(\alpha\beta) + \frac{1}{\beta}\, lnt$$

Where q_t is the amount of dye adsorbed (mg/g) at time (t), α represents the initial sorption rate (mg g^{-1} $min^{-}1$) and α is related to the extent of surface coverage and activation energy for chemisorption (g mg^{-1}). On plotting Equation 5 (Figure 10) no straight lines are observed for the different initial concentrations. The parameters α, β and the correlation coefficients R^2 are calculated from the plots and consigned in Table 1. The whole correlation coefficients were lower than the unit. This model is not suitable to study the sorption of fuschin basic on leaves of *Datura stramonium*. The sorption process of fuschin basic on powder leaves of *Datura stramonium* is best described by the pseudo-second-order model as shown by the parameter's values consigned in Table 1.

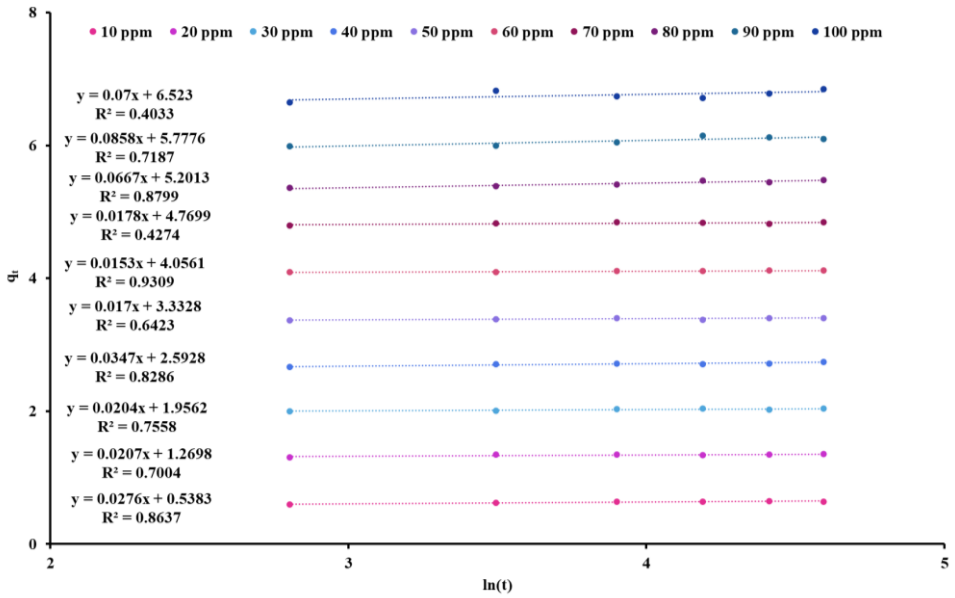

Figure 10. Elovich kinetic model for adsorption of fuschin basic on DSL.

Table 2. Adsorption isotherms parameters

Langmuir isotherm			**Freundlich isotherm**		
$\frac{C_e}{q_e} = \frac{1}{K_L Q_0} + \frac{1}{Q_0} C_e$			$\ln q_e = \ln K_F + \frac{1}{n} \ln C_e$		
Q_0 (mg/g)	K_L (L/mg)	R^2	$\frac{1}{n}$	K_F	R^2
− 8.230	− 0.125	0.262	1.374	1.068	0.902
Temkin isotherm			**Dubinin-Raduskevich**		
$q_e = \frac{RT}{b_t} \ln K_T + \frac{RT}{b_t} \ln C_e$			$\ln q_e = \ln Q_{max} - B_D \varepsilon^2$		
bt	K_T	R^2	Q_{max}	BD	R^2
630.743	1.281	0.949	7.550	7×10^{-7}	0.965
Harkin-Jura			**Halsey**		
$\frac{1}{q_e^2} = \frac{B_{HJ}}{A_{HJ}} - \frac{1}{A_{HJ}} \log C_e$			$\ln q_e = \frac{1}{n_H} \ln K_H - \frac{1}{n_H} \ln C_e$		
A_{HJ}	B_{HJ}	R^2	n_H	K_H	R^2
− 0.447	− 0.467	0.478	− 0.728	0.896	0.902

Isotherms

The way in which adsorbate molecules are distributed between the liquid phase and the solid adsorbent can be described by studying the relationship between the amount of adsorbate adsorbed at equilibrium and the equilibrium adsorbate concentration. These phenomena can be described by mathematical models called adsorption isotherms. The experimental data are analyzed by fitting them to different models. To find the best model for design purposes, isotherm models named Langmuir [31], Freundlich [32], Temkin [33], Dubinin-Raduskevich [34], Harkin-Jura [35] and Halsey [36] were used. The equations which describes the models are reported in our previous work [26, 37]. The constants were determined from the plots of relative equations and the isotherm parameters as presented in Table 2. Figure 11 shows the Langmuir, Freundlich, Temkin, Dubinin-Raduskevich, Harkin-Jura and Halsey curves adsorption of fuschin basic on *Datura stramonium* leaves powder. The Langmuir and Harkin-Jura models are the least suitable for the experimental equilibrium adsorption data of basic fuschin with low correlation coefficients R^2 of 0.262 and 0.478, respectively. It is observed that the Freundlich and Halsey isotherms are quite suitable for the description of the adsorption of basic fuschin by *Datura stramonium* leaf powder with identical correlation coefficients R^2 of 0.902 for both isotherms. The experimental adsorption data of basic fuschin were fitted by the Temkin model with a fairly good correlation coefficient of 0.949. The Dubinin-Raduskevich isotherm is also suitable for describing the adsorption of basic fuschin on *Datura stramonium* leaf powder with a correlation coefficient R^2 of 0.965. These observations suggest that the adsorption system is heterogeneous.

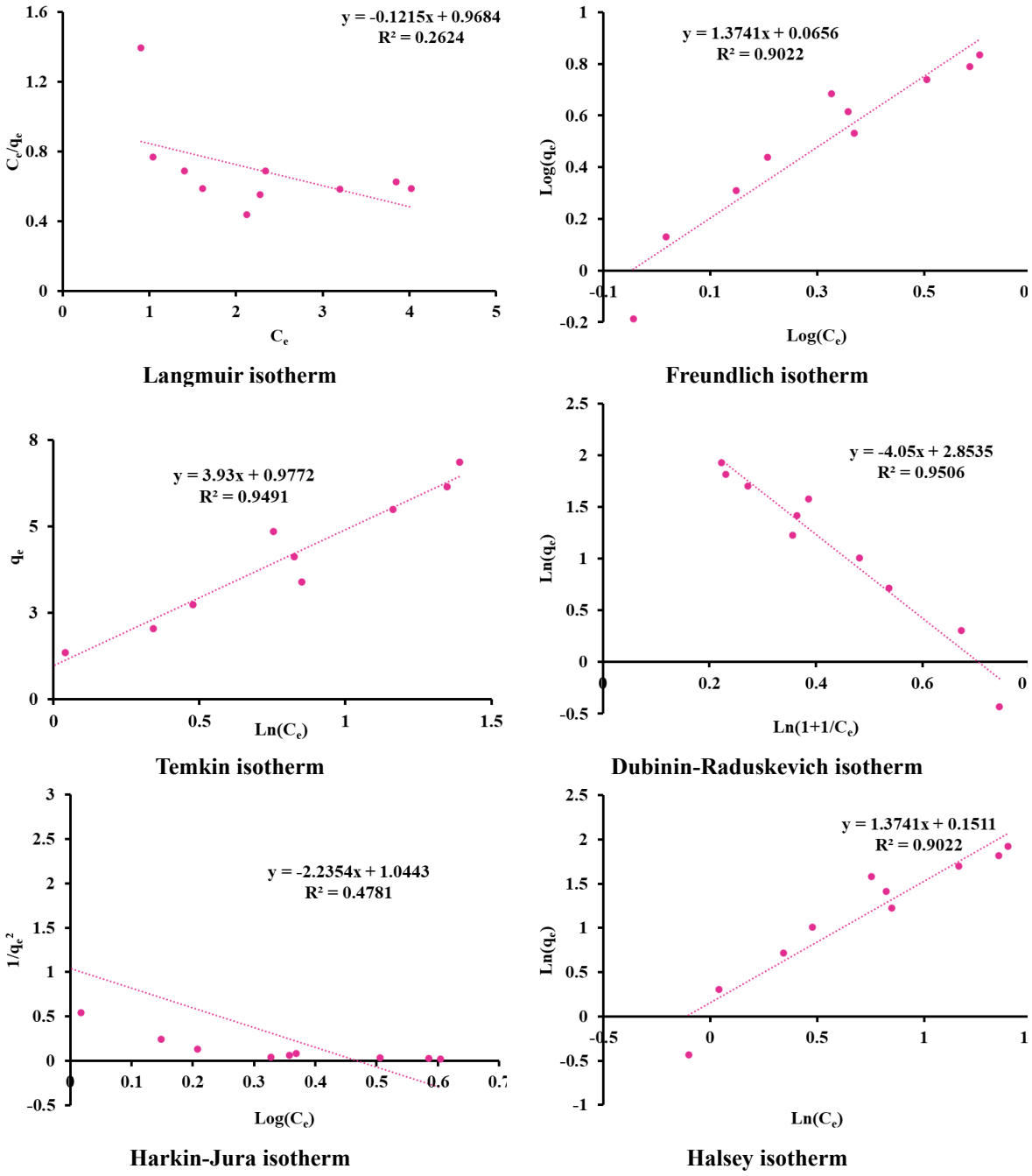

Figure 10. Adsorption isotherms of fuschin basic on *Datura stramonium* leaf powder.

IV.Conclusion

In this paper, *Datura Stramonium* leaves were used for the decontamination of wastewater containing basic fuschin. FTIR analysis and zero-point loading were performed to determine the properties of the adsorbent. The equilibrium stirring time for fuschin basic sorption is 60 minutes. The optimal dosage for sorption is 14 g/L and the optimal size of the adsorbent is 125 µm. The optimal initial concentration of basic fuschin is 70 ppm. The sorption percentage of basic fuschin from the aqueous solution changes significantly with increasing pH, from 2 (90.54%) to 11 (82.63%), with a maximum at pH 5 (95.28%). The adsorption kinetics was well described by the pseudo-second-order model, proving that chemisorption would be the rate-controlling step. The adsorption isotherms of basic fuschin fit fairly well to the Temkin and Dubinin-Raduskevich models with correlation coefficients of 0.949 and 0.965, respectively. The short contact time (60 minutes), low adsorbent-to-volume ratio (0.014), and pH of 5 obtained to achieve the maximum adsorption capacity demonstrate that the prepared adsorbent is a durable, low-cost, and highly efficient absorbent that can be used to remove industrial dyes from wastewater. The recycling of the adsorbent and its affinity for other industrial dyes, as well as its performance for

highly contaminated wastewater, should be investigated to consider the use of *Datura Stramonium* powder on a larger scale.

References

[1]. Renita, A. A., Kumar, P. S., & Jabasingh, S. A. (2019). Redemption of acid fuchsin dye from wastewater using de-oiled biomass: Kinetics and isotherm analysis. *Bioresource Technology Reports*, *7*, 100300. https://doi.org/10.1016/j.biteb.2019.100300

[2]. El-Azazy, M., El-Shafie, A. S., Ashraf, A., & Issa, A. A. (2019). Eco-Structured biosorptive removal of basic fuchsin using pistachio nutshells: A definitive screening design—based approach. *Applied Sciences*, *9*(22), 4855. https://doi.org/10.3390/app9224855

[3]. Foroutan, R., Peighambardoust, S. J., Boffito, D. C., & Ramavandi, B. (2022). Sono-Photocatalytic Activity of Cloisite 30B/ZnO/Ag_2O Nanocomposite for the Simultaneous Degradation of Crystal Violet and Methylene Blue Dyes in Aqueous Media. *Nanomaterials*, *12*(18), 3103. https://doi.org/10.3390/nano12183103

[4]. Bansal, M., Pal, B., & Das, R. K. (2024). Improved adsorption of Fuschin Blue with Sn^{2+} impregnated Zn-Bi mixed metal hydroxide. *Next Sustainability*, *4*, 100060. https://doi.org/10.1016/j.nxsust.2024.100060

[5]. Hu, M., Wang, X., Wang, C., Chu, H., Song, X., Dong, G., Zhang, J., & Xing, J. (2025). Synthesis and structure characterization of boron complexes containing C2-symmetric tertiary amine ligands: Assessment catalytic degradation of dyes and antioxidant properties. *Journal of Molecular Structure*, *1334*, 141842. https://doi.org/10.1016/j.molstruc.2025.141842

[6]. Kader, D. A., Abdalla, S. A., Mohammed, S. J., Aziz, D. M., Ghafoor, D. D., Abdullah, T. M., Agha, N. N. M.0, Mustafa, F. S. & Hassan, S. A. (2025). Green Light, green Chemistry: TiO_2@PPHs nanocomposite for Eco-Friendly photocatalytic oxidation of amines and degradation of Brilliant green dye. *Journal of Photochemistry and Photobiology A: Chemistry*, *462*, 116253. https://doi.org/10.1016/j.jphotochem.2024.116253

[7]. Padervand, M., Bargahi, A., Eftekhari-Sis, B., Saadi, M., Ghasemi, S., Dawi, E. A., Labidi, A., Mahmoudi, G., & Gargari, M. S. (2024). In-situ synthesis of SnO/$CuSnO_3$ nanostructures to catalyze azo dye degradation, CO_2 reduction, and amines direct alkylation reactions under visible light. *Results in Engineering*, *23*, 102515. https://doi.org/10.1016/j.rineng.2024.102515

[8]. Gupta, V. K., Mittal, A., Gajbe, V., & Mittal, J. (2008). Adsorption of basic fuchsin using waste materials—bottom ash and deoiled soya—as adsorbents. *Journal of Colloid and Interface Science*, *319*(1), 30–39. https://doi.org/10.1016/j.jcis.2007.09.091

[9]. Littlefield, N. A., Blackwell, B.-N., Hewitt, C. C., & Gaylor, D. W. (1985). Chronic Toxicity and Carcinogenicity Studies of Gentian Violet in Mice. *Fundamental and Applied Toxicology*, *5*(5), 902–912. https://doi.org/10.1093/toxsci/5.5.902

[10]. Vinayagam, R., Kar, A., Murugesan, G., Varadavenkatesan, T., Goveas, L. C., Samanth, A., Ahmed, M. B., & Selvaraj, R. (2023). Low temperature carbonized mesoporous graphitic carbon for tetracycline adsorption: Mechanistic insight and adaptive neuro-fuzzy inference system modeling. *Bioresource Technology Reports*, *22*, 101468. https://doi.org/10.1016/j.biteb.2023.101468

[11]. Bhattacharyya, K. G., & Sharma, A. (2005). Kinetics and thermodynamics of Methylene Blue adsorption on Neem (Azadirachta indica) leaf powder. *Dyes and Pigments*, *65*(1), 51–59. https://doi.org/10.1016/j.dyepig.2004.06.016

[12]. Kannan, N., & Sundaram, M. M. (2001). Kinetics and mechanism of removal of methylene blue by adsorption on various carbons—a comparative study. *Dyes and Pigments*, *51*(1), 25–40. https://doi.org/10.1016/S0143-7208(01)00056-0

[13]. Islam, M. A., Nazal, M. K., Akinpelu, A. A., Sajid, M., Alhussain, N. A., Billah, R. E. K., & Bahsis, L. (2024). Novel activated carbon derived from a sustainable and low-cost palm leaves biomass waste for tetracycline removal: Adsorbent preparation, adsorption mechanisms and real application. *Diamond and Related Materials*, *147*, 111375. https://doi.org/10.1016/j.diamond.2024.111375

[14]. Vinayagam, R., Quadras, M., Varadavenkatesan, T., Debraj, D., Goveas, L. C., Samanth, A., Balakrishnan, D., & Selvaraj, R. (2023). Magnetic activated carbon synthesized using rubber fig tree leaves for adsorptive removal of tetracycline from aqueous solutions. *Environmental Research*, *216*, 114775. https://doi.org/10.1016/j.envres.2022.114775

[15]. Martins, A. C., Pezoti, O., Cazetta, A. L., Bedin, K. C., Yamazaki, D. A. S., Bandoch, G. F. G., Asefa, T., Visentainer, J. V., & Almeida, V. C. (2015). Removal of tetracycline by NaOH-activated carbon produced from macadamia nut shells: Kinetic and equilibrium studies. *Chemical Engineering Journal*, *260*, 291–299. https://doi.org/10.1016/j.cej.2014.09.017

[16]. Bhattacharyya, K. G., & Sharma, A. (2005). Kinetics and thermodynamics of Methylene Blue adsorption on Neem (Azadirachta indica) leaf powder. *Dyes and Pigments*, *65*(1), 51–59. https://doi.org/10.1016/j.dyepig.2004.06.016

[17]. Khatooni, H., Peighambardoust, S. J., Foroutan, R., Mohammadi, R., & Ramavandi, B. (2023). Adsorption of methylene blue using sodium carboxymethyl cellulose-g-poly (acrylamide-co-methacrylic acid)/Cloisite 30B nanocomposite hydrogel. *Journal of Polymers and the Environment*, *31*(1), 297–311. https://doi.org/10.1007/s10924-022-02623-x

[18]. Vardhan, K. H., Kumar, P. S., & Panda, R. C. (2019). A review on heavy metal pollution, toxicity and remedial measures: Current trends and future perspectives. *Journal of Molecular Liquids*, *290*, 111197. https://doi.org/10.1016/j.molliq.2019.111197

[19]. Wu, X., Cobbina, S. J., Mao, G., Xu, H., Zhang, Z., & Yang, L. (2016). A review of toxicity and mechanisms of individual and mixtures of heavy metals in the environment. *Environmental Science and Pollution Research*, *23*(9), 8244–8259. https://doi.org/10.1007/s11356-016-6333-x

[20]. Wang, S., Zhang, L., Zhao, C., Liu, G., Zhou, H., Dai, W., Zhang, Y., Cui, C., & Huang, S. (2024). Hybrid capacitive deionization from a nickel hexacyanoferrate/biomass derived porous carbon toward enhanced sodium adsorption for water desalination. *Journal of Water Process Engineering*, *68*, 106508. https://doi.org/10.1016/j.jwpe.2024.106508

[21]. Nand, S., Kumar, S., Pratap, B., Dubey, D., Naseem, M., Patel, A., Shukla, S., & Srivastava, P. K. (2024). Arsenic removal using de-oiled mentha biomass biochar: Adsorption kinetics and the role of iron modification. *Journal of Cleaner Production*, *482*, 144247. https://doi.org/10.1016/j.jclepro.2024.144247

[22]. Zheng, B., He, Y., Tian, S., Wang, S., & Tang, L. (2025). Bamboo fiber-reinforced chitosan biomass aerogel for Cr(VI) and Cu(II) capture: Batch adsorption experiments and density functional theory calculations. *Applied Surface Science*, *703*, 163391. https://doi.org/10.1016/j.apsusc.2025.163391

[23]. Karadirek, Ş., Kanmaz, N., Tuna, Ö., & Demircivi, P. (2025). Designing of N/O heteroatoms doped biomass-derived activated carbon for boosting toxic dye pollutant adsorption. *Biomass and Bioenergy*, *199*, 107968. https://doi.org/10.1016/j.biombioe.2025.107968

[24]. Fernández-Andrade, K. J., Fernández-Andrade, A. A., Arteaga-Pérez, L. E., & Rodriguez-Diaz, J. M. (2025). Dataset on the synthesis, characterization, and application of MIL-53(Al)@Biomass hybrid for efficient oxytetracycline elimination via adsorption and photocatalysis. *Data in Brief*, *60*, 111628. https://doi.org/10.1016/j.dib.2025.111628

[25]. Akinyeye, O. J., Ibigbami, T. B., & Odeja, O. (2016). Effect of Chitosan Powder Prepared from Snail Shells to Remove Lead (II) Ion and Nickel (II) Ion from Aqueous Solution and Its Adsorption Isotherm Model. *American Journal of Applied Chemistry*, *4*(4), 146–156.

https://doi.org/10.11648/j.ajac.20160404.15
[26]. Gaye, A. A., Diouf, R., & Fall, A. (2023). Bio-sorption of Methylene Blue by Defatted Seed of Adansonia digitata. *Earthline Journal of Chemical Sciences*, *9*(1), 139–156. https://doi.org/10.34198/ejcs.9123.139156
[27]. Shahwan, T. (2015). Lagergren equation: Can maximum loading of sorption replace equilibrium loading? *Chemical Engineering Research and Design*, *96*, 172–176. https://doi.org/10.1016/j.cherd.2015.03.001
[28]. Aichour, A., & Zaghouane-Boudiaf, H. (2019). Highly brilliant green removal from wastewater by mesoporous adsorbents: Kinetics, thermodynamics and equilibrium isotherm studies. *Microchemical Journal*, *146*, 1255–1262. https://doi.org/10.1016/j.microc.2019.02.040
[29]. Weber, W. J., & Morris, J. C. (1963). Kinetics of Adsorption on Carbon from Solution. *Journal of the Sanitary Engineering Division*, *89*(2), 31–59. https://doi.org/10.1061/JSEDAI.0000430
[30]. Cope, F. W. (1972). Generalizations of the Roginsky-Zeldovich (or Elovich) equation for charge transport across biological surfaces. *The bulletin of mathematical biophysics*, *34*(3), 419–427. https://doi.org/10.1007/BF02476452
[31]. Marczewski, A. W. (2010). Analysis of Kinetic Langmuir Model. Part I: Integrated Kinetic Langmuir Equation (IKL): A New Complete Analytical Solution of the Langmuir Rate Equation. *Langmuir*, *26*(19), 15229–15238. https://doi.org/10.1021/la1010049
[32]. Debnath, S., & Das, R. (2023). Strong adsorption of CV dye by Ni ferrite nanoparticles for wastewater purification: Fits well the pseudo second order kinetic and Freundlich isotherm model. *Ceramics International*, *49*(10), 16199–16215. https://doi.org/10.1016/j.ceramint.2023.01.218
[33]. Araújo, C. S. T., Almeida, I. L. S., Rezende, H. C., Marcionilio, S. M. L. O., Léon, J. J. L., & Matos, T. N. de. (2018). Elucidation of mechanism involved in adsorption of Pb(II) onto lobeira fruit (Solanum lycocarpum) using Langmuir, Freundlich and Temkin isotherms. *Microchemical Journal*, *137*, 348–354. https://doi.org/10.1016/j.microc.2017.11.009
[34]. Ghezini, R., Sassi, M., & Bengueddach, A. (2008). Adsorption of carbon dioxide at high pressure over H-ZSM-5 type zeolite. Micropore volume determinations by using the Dubinin–Raduskevich equation and the "t-plot" method. *Microporous and Mesoporous Materials*, *113*(1), 370–377. https://doi.org/10.1016/j.micromeso.2007.11.034
[35]. Erdogan, F. O. (2019). Freundlich, Langmuir, Temkin, DR and Harkins-Jura Isotherm Studies on the Adsorption of CO_2 on Various Porous Adsorbents. *International Journal of Chemical Reactor Engineering*, *17*(5), 20180134. https://doi.org/doi:10.1515/ijcre-2018-0134
[36]. Halsey, G. D. (1952). The Role of Surface Heterogeneity in Adsorption. In W. G. Frankenburg, V. I. Komarewsky, & E. K. Rideal (Eds.), (Vol. 4, pp. 259–269). Academic Press. https://doi.org/10.1016/S0360-0564(08)60616-1
[37]. Dior Samb, D., Gaye, A. A., & Fall, A. (2022). Bio-sorption of Methylene Blue by Euphorbia hirta leaves. *IOSR Journal of Environmental Science, Toxicology and Food Technology (IOSR-JESTFT)*, *16*(6), 9–18. https://doi.org/10.9790/2402-1606010918